Title
EXPERIMENTAL STATUS OF THE LEADING NON-STRANGE MESON TRAJECTORIES

Author
Gidal, George.

Publication Date
1971-09-01

Invited paper presented at the Annual Meeting of the Division of Particles and Fields, University of Rochester, Rochester, NY August 30 - September 2, 1971

LBL-352
Preprint c.2

EXPERIMENTAL STATUS OF THE LEADING NON-STRANGE MESON TRAJECTORIES

George Gidal

September 1971

AEC Contract No. W-7405-eng-48

I have been asked to summarize the current experimental situation concerning the leading non-strange Regge trajectories. The ultimate goal, of course, is to use the experimental data to determine all the amplitudes for a given reaction, but such a goal has only approximately been achieved in the case of the well-studied elastic scattering. I refer you to G. Fox's talk[1] at the Cal Tech Conference for a summary of the latest word in amplitude phenomenology. We shall here limit ourselves to a summary of the gross structure over a large interval of momentum transfer. We shall further limit ourselves to those reactions or combinations of reactions which <u>isolate a single leading trajectory</u> in the t channel. We assume the validity of the Regge theory with nonsense wrong signature zeroes (NWSZ) and use the formula

$$d\sigma/dt\ (\nu, t) = G(t)\ \nu^{2\alpha_{eff}-2}$$

together with the positions of the NWSZ dips to provide information about the trajectory, and rely on the internal consistency of the data to justify these assumptions. In general, several helicity amplitudes contribute to a given reaction, each with a different ν dependence, necessitating corrections to the α_{eff}, but we neglect this effect considering the present state of the data. We are aware of the known necessity of introducing lower lying trajectories, absorptive corrections and/or Regge cuts into NWSZ models but these will also be ignored. For justification we appeal to the observation that amplitudes which have a single unit of helicity flip in the s channel (n=1) are least subject to such corrections.[2] Most of the reactions we comment on here satisfy this condition. We emphasize that much of the data comes from πN interactions at intermediate energies (2 - 5 GeV/c) since Regge shrinkage makes the best statistics at large $|t|$ available here. Photoproduction reactions will not be considered.

We will discuss:

I. Reactions in which only one leading trajectory can be exchanged (ρ, A_2)

II. Reactions in which we can isolate the leading trajectory by Isospin (P^I, ω^o, f^o)

III. Reactions in which we can isolate the leading trajectory by Parity (B).

I. The classic example of the success of the Regge model is, of course, the $\pi^- p \to \pi^o n$ charge exchange reaction. New measurements[3] at large momentum transfers by the Case Western Reserve group at Argonne have enabled us to extend the α_{eff} analysis to large $|t|$. In Figure I we show a compilation of Barger and Phillips[4] which includes this data, superimposed on $\alpha_{eff} = 0.55 + t$. This reaction also forms part of the elastic πN scattering trio and a recent measurement of the $\dot{R}$ parameter[5] has allowed a model independent determination of the amplitude at 6 GeV/c. We shall talk more about this but now mention only that while a pure ρ exchange model is obviously wrong, as witnessed by the observed polarization, it is actually not far from the truth. The NWSZ dip, corresponding in this case of an odd signature trajectory to the value of t for which $\alpha = 0$, is seen at all energies[6] near $t = -0.6$. This dip is also observed in the reaction $\pi^+ p \to \pi^o \Delta^{++}$ at several energies.[7] We remind you of this data in Figs. 2 and 3.

The only other class of reactions believed to be dominated by the exchange of a single leading trajectory is eta production, $\pi^- p \to \eta^o n$ and $\pi^+ p \to \eta^o \Delta^{++}$. For many years the A_2 trajectory as determined from the reaction $\pi^- p \to \eta^o n$ was thought to be shallower than the ρ trajectory.[8] About a year ago we[9] determined this trajectory from the reaction $\pi^+ p \to \eta^o \Delta^{++}$ with the results shown in Fig. 4. The best fit value, $\alpha_{eff} = 0.87 + 1.75\ t$, is considerably steeper than the old A_2 trajectory, $\alpha_{eff} = .34 + .35\ t$, while the chi-squared for a trajectory degenerate with the ρ trajectory is not too bad. Subsequently, the $\eta^o n$ data was reanalyzed by Spiro and Derem[10] who showed that the effective trajectory became steeper as one included only higher energy data, perhaps due to the presence of s-channel effects. We have since redone the detailed <u>Regge amplitude fit</u>[11] of Krammer and Maor for $\pi^+ p \to \eta^o \Delta^{++}$ at momenta between 2.3 and 8 GeV/c and find a best fit with $\alpha = 0.58 + 1.01\ t$. That this is not the same as the α_{eff} previously shown as a best fit, is due to the additional constraint on the form of G(t) and to the different ν dependence of the contributing amplitudes (chi-squared = 120 for 90 DF). To test the reliability of such a Regge fit at intermediate energies we have partial wave analyzed these best fit Regge amplitudes and show the result in comparison with our measurements of this reaction down to threshold in Fig. 5. The agreement is remarkable and indicates the absence of important s channel contributions.

Another test of the model is provided by the existence and position of the NWSZ dip of this even signature trajectory corresponding to the value of t at which $\alpha = -1$. Again, from the paper[9] of Grether and myself, we show in Fig. 6 the differential cross section summed over several energies, and clearly see the predicted minimum near $t = -1.5$. More recently two other experiments have observed this dip in the reaction $\pi^- p \to n^o n$. The Minnesota group[12] and the Case Western Reserve group,[13] in complementary experiments at Argonne, have measured the differential cross section over a very large t interval at 3.65 GeV/c and we show their data on the same graph in Fig. 7. The MIT group[14] has also recently reported this dip at many momenta between 1.4 and 3.8 GeV/c. We show their graph of dip position in the Mandelstam plane in Fig. 8.

II. We consider three examples in which we can isolate leading trajectories from a separation into $I = 0$ and $I = 1$ exchanges in the t channel. Take reactions of the type $\pi N \to M N$ where M is an isovector meson (ρ, π, A_2). Since the $I = 1$ component of the amplitude changes sign under charge conjugation and the $I = 0$ component does not, the amplitudes are

$$T(\pi^{\pm} p \to m^{\pm} p) \sim (T^{0} \mp T^{1}) \equiv T_{\pm}$$

$$T(\pi^{-} p \to m^{o} n) \sim \sqrt{2}\, T^{1} \qquad \equiv T_{o}$$

The superscript refers to I_t while the subscript refers to the meson charge.

$$|T^0|^2 = \frac{1}{2}\{|T_+|^2 + |T_-|^2 - |T_o|^2\} \equiv X(t)$$

$$|T^1|^2 = \frac{1}{2}|T_o|^2$$

$$\cos\theta = \frac{\vec{T}^0 \cdot \vec{T}^1}{|T^0||T^1|} = \frac{|T_+|^2 - |T_-|^2}{4|T^0||T^1|}$$

The most complete study of such a decomposition has, of course, been done with elastic pion nucleon scattering. A recent work of Halzen and Michael[15] has provided a model independent determination of the amplitudes at 6 GeV/c. In this case the I = 1 component is the previously discussed ρ trajectory, while the I = 0 component contains P and P'. We show the result of this amplitude determination for the I = 1 component in Fig. 9 together with the results of a previous Regge pole fit of Barger and Phillips[16] indicating that their model is a very good fit. This shows again that the NWSZ dip near t = -.6 comes from the I_t = 1 spin flip amplitude. More recently, Barger and Phillips[4] have done this decomposition with the newer large angle data and we show separately their I = 1 and I = 0 differential cross sections in Fig. 10. They note that the dips at large $|t|$ values appear in the I_t = 0 component, perhaps corresponding to the $\alpha = -2$ and $\alpha = -4$ intercepts of the P' trajectory. Here, of course, the polarization in $\pi^{\pm}p$ elastic scattering comes from the interference between the I = 0 and I = 1 exchanges.

In a contribution to this conference,[17] Michael, Grether, and I have applied the same analysis to the reaction $\pi N \to \rho N$ as was first suggested by Contigouris, Tran Thanh Van and Lubbatti.[18] In this case the $I = 0$ exchange can only be the ω^o trajectory, while the $I = 1$ exchange consists of at least π and A_2 exchange.

We show first in Fig. 11 our measurement of $d\sigma/dt$ for $\pi^+p \to \rho^+p$ at 2.67 GeV/c. This was obtained with a maximum likelihood fit of the Dalitz plot in each interval of t with the known major final states, eliminating the usual uncertainty in background subtraction. This method is especially advantageous in obtaining the decay angular distributions of the rho.

Fortunately the best measurement of the reactions $\pi^-p \to \rho^-p$ and $\pi^-p \to \rho^on$ over a wide range of momentum transfers is at 2.77 GeV/c,[19] an energy very close to our own. We then show in Fig. 12 the combination $X(t) = |T^o|^2$. The coarser intervals of the published π^-p work make it difficult to draw any conclusions about the behavior at very small t (a flattening is already apparent in this data), but a clear dip near $t = -0.4$ is observed. While the actual magnitude of this ω^o exchange contribution is subject to uncertainties in the normalizations of the two experiments, the position of the dip is insensitive to a wide range of relative normalizations. This dip occurs at $t = -0.40 \pm 0.05$ GeV/c^2 and, in a nonsense wrong signature zero model, is interpreted as the value of t at which the ω^o trajectory passes through zero. In Fig. 13 we show this point together with the other available data concerning the ω^o trajectory. In addition to the ω^o mass, a recent SLAC measurement[20] of $\alpha_\omega(0) = 0.47 \pm 0.09$ from the reaction $K_L^op \to K_S^op$, and the result of earlier fits to the total cross sections,[21] $\alpha(0) = 0.38 \pm 0.04$ are shown. The straight line is $\alpha = 0.4 + t$, lying somewhat lower than the commonly accepted trajectory, $\alpha_\rho = 0.57 + .91t$. Reliable measurements of X(t) at several values of s would provide additional points on the ω^0 trajectory.

One can also obtain the phase between the I = 0 and I = 1 amplitudes from the relation

$$\cos\theta = \vec{T}^0 \cdot \vec{T}^1/|T^0||T^1| = (|T_+|^2 - |T_-|^2)/(4|T^0||T^1|)$$

and we show this phase in Fig. 14 for our reactions. While the amplitudes are approximately incoherent at small momentum transfers, coherence sets in after the dip. Such measurements are, however, extremely sensitive to normalizations.

An alternative explanation is offered by Strong Absorption models.[32] If zero helicity ρ's come only from pion exchange and if this exchange flips the proton helicity in the s channel (n = 1), such models predict a dip in $\rho_{00}^H\, d\sigma/dt$ near t = -0.5. This is exactly what is observed in Fig. 15 but we note that ρ_{00} itself has a smooth behavior in this region, so that this is probably the same dip observed in $d\sigma/dt$.

The same considerations can be applied to A_2 production, and have been summarized by Rosner[23] and Michael.[24] Unfortunately, the best data is in the $\rho\pi$ decay mode which has a large background. The total cross section data show that the I = 0 exchange dominates, accounting for almost 3/4 of the cross section. Now the $I_t = 0$ exchange is the f^0 while the $I_t = 1$ exchange is the ρ with perhaps a bit of π and B. This is confirmed by the fact that in all decay modes $\rho_{11} \sim \rho_{1-1} \sim 0.4$ so that natural parity exchange dominates. We show the differential cross sections[25] presented at the Cal Tech Conference in Figs. 16 and 17. As expected, for an even signature trajectory the only evidence for a dip comes above t = -1. The odd signature ρ trajectory will only contribute to A_2^o production and one might expect a dip near t = -.6 for such reactions. Barnham et al.[26] have reported a lack of A_2 signal in this t interval in the $\pi^+ p \to A_2^o \Delta^{++}$ final state at 3.7 GeV/c but the data are very sparse. In general we need good data in the ηπ decay mode over a large t interval. The Illinois group[27] has concluded from the near equality of the A_2^+ and A_2^- cross sections that there is no coherence between $I_t = 0$ and $I_t = 1$ amplitudes.

III. For reactions of the type $\pi N \to VN$ in which the vector meson decay is expressed in terms of the density matrix elements, ρ_{ij}, remember that $\rho_{oo} + 2\rho_{11} = 1$ so that we can write

$$d\sigma/dt = d\sigma/dt\,(\rho_{oo}+2\rho_{11}) = \underset{(\mathrm{Hel}\,=\,0)}{\rho_{oo}\,d\sigma/dt} + \underset{(\mathrm{Hel}\,=\,\pm 1)}{2\rho_{11}\,d\sigma/dt}$$

which separates the cross section into a part corresponding to vector meson having helicity = 0 and a part corresponding to helicity = ± 1. Gottfried and Jackson[28] showed that natural parity exchange does not populate the t channel helicity = 0 state, i.e. $\rho_{oo}^t\,d\sigma/dt$ measures helicity non-flip unnatural parity exchange independent of s. Rewrite as

$$d\sigma/dt = \rho_{oo}\,d\sigma/dt + (\rho_{11}-\rho_{1-1})\,d\sigma/dt + (\rho_{11}+\rho_{1-1})\,d\sigma/dt$$

Ader et al.[29] have shown that to order 1/s in both s- and t-channel frames,[30]

$\rho_{oo}\,d\sigma/dt$ measures the helicity non-flip unnatural parity exchange;

$(\rho_{11} - \rho_{1-1})\, d\sigma/dt$ measures the helicity flip unnatural parity exchange;

$(\rho_{11} + \rho_{1-1})\, d\sigma/dt$ measures the helicity flip natural parity exchange.

We will here consider the example of the reactions $\pi^+ n \to \omega^o p$ and $\pi^+ p \to \omega^o \Delta^{++}$. It is already well established that the differential cross section has no dip near $t = -0.6$ and that ρ_{oo} is sizeable,[31] both indicating that rho exchange is not the only contributing amplitude. The prime candidate for the unnatural parity contribution is the B trajectory. We show in Fig. 18 a compilation of some of the better statistics experiments[32] (not meant to be complete) of ρ^{t}_{oo}. The common feature apart from the finite size is the appearance of a dip structure in the region of $t = -0.2$ in most experiments. We note, however, that in some experiments this is a very narrow dip while in others it is quite broad. $d\sigma/dt$ is usually structureless in this t region. If we take this dip as the NWSZ of the B trajectory (being an odd signature trajectory, the point where $\alpha_B = 0$) and require a linear trajectory passing through the B meson mass, then $\alpha_B(t) = 0.12 + 0.59\, t$.

Tran Thanh Van and collaborators[33] have obtained reasonable amplitude fits to the reaction $\pi^+ n \to \omega^o p$ with such a trajectory and we show their fit to the s dependence in Fig. 19. We[35] have done a fit of α_{eff} for the $\pi^+ p \to \omega^o \Delta^{++}$ data (see Figs. 20 and 21) and obtain $\alpha_{B_{eff}} = (.15 \pm .12) + (.62 \pm .23)\, t$, in excellent agreement (considering all the amplitudes involved) with the trajectory hypothesized from the dip position. Since the data is still rather poor, this interpretation is subject to considerable doubt. In fact, Mathews and Muen[34] have also obtained a reasonable amplitude fit to this reaction with $\alpha_B = -0.2 + 0.8\ t$. An alternative trajectory which assumes π-B exchange degeneracy has been successfully used by Abrams and Maor[36] in fitting $\pi^+p \rightarrow \rho^o\Delta^{++}$, $\omega^o\Delta^{++}$ and $K^+p \rightarrow K^{*o}\Delta^{++}$. They use the trajectory function $\alpha(t) \approx 1.12\ t$ and are able to reproduce both the s and t dependence of these reactions quite well. Pols et al.[37] have obtained a reasonable fit to this model at 5 GeV/c with $\alpha(t) \approx 1.17\ t$. In a contribution to this conference, the Toronto group[38] has repeated this fit to new data at 5.45 GeV/c and find they need a rather steeper trajectory, $\alpha(t) \approx 1.34\ t$, to fit the data. The results of these fits are summarized in Fig. 22. That this model also provides a decent fit with so different a trajectory than the α_{eff} determined directly is again due to the assumption of a specific form of the amplitude, i.e., a specific form of G(t) which is not the best fit but an acceptable fit. Clearly precise data at larger s and t, and a clarification of the nature of the dip near t = -.2, are needed to extract the B trajectory.

Work performed under the auspices of the U.S. Atomic Energy Commission.

References

1. G. Fox, Phenomenology in Particle Physics 1971, Calif. Institute of Technology, Pasadena, Calif.
2. C. Chiu, Proceedings of Workshop in Particle Physics at Intermediate Energies, Pasadena, 1971; also CALT-68-300.
3. W. S. Brockett et al., Phys. Rev. Lett. 26, 527 (1971).
4. V. Barger and R. J. N. Phillips, Wisconsin Preprint, 1971.
5. B. Amblard, Thesis, University of Paris, 1971; CNRS-AO-5421.
   P. Bonamy et al., Phys. Lett. 23, 501 (1966).
6. S. Sonderegger et al., Phys. Lett. 20, 75 (1966).
7. G. Gidal, et al., Phys. Rev. Lett. 23, 994 (1969).
8. R. J. N. Phillips and W. Rarita, Phys. Lett. 19, 598 (1965).
9. D. Grether and G. Gidal, Phys. Rev. Lett. 26, 792 (1971).
10. Spiro and Derem, Lett. al Nuovo Cimento, Vol. 1, No. 3, 81 (1971).
11. D. Grether and G. Gidal, to be published.
12. E. H. Harvey et al., University of Minnesota Preprint, 1971.
13. A. R. Kirby et al., Bulletin of American Physical Society 16, 634 (1971); private communication.
14. Cambridge Bubble Chamber Group (Brown, Harvard, MIT, Padova and Weizmann) - paper submitted to Amsterdam Conference, June 1971.
15. F. Halzen and C. Michael, CERN Th.1355, 1971.
16. V. Barger and R. J. N. Phillips, Phys. Rev. 187, 2210 (1969).
17. W. Michael, D. Grether and G. Gidal, The Reaction $\pi^+ p \to \rho^+ p$ at 2.67 GeV/c - paper submitted to 1971 Annual Meeting of the Division of Particles and Fields.
18. A. P. Contogouris, J. Tran Thanh Van, H. J. Lubatti, Phys. Rev. Lett. 19, 1352 (1967).

19. J. P. Baton and G. Laurens, Nuclear Physics B21, 551 (1970).

20. A. D. Brody et al., Phys. Rev. Lett. 26, 1050 (1971).

21. V. Barger et al., Nucl. Phys. B5, 411 (1968).

22. M. Ross, F. J. Henyey, and G. L. Kane, Nucl. Phys. B23, 269 (1970).

23. J. Rosner, Phenomenology in Particle Physics 1971, Calif. Institute of Tech., Pasadena, 1971.

24. C. Michael and P. V. Ruuskanen, CERN Th.1308, 1971.

25. K. Lai, Phenomenology in Particle Physics 1971, Calif. Inst. of Tech., Pasadena, 1971.

26. K. W. Barnham, et al., UCRL-20050, Contribution to XVth International Conference on High Energy Physics, Kiev, 1970.

27. D. V. Brockway et al., Univ. of Illinois preprint COO-1195-202 Contribution to Austin Meeting of the Division of Particles and Fields, 1970.

28. K. Gottfried and J. D. Jackson, Nuovo Cimento 33, 309 (1964).

29. J. P. Ader, M. Capdeville, G. Cohen-Tannoudji, Ph. Salin, Nuovo Cimento 56A, 952 (1968).

30. For a concise summary of the relations between s-channel and t-channel density matrix elements, see D. Grether, P-B 178 Lawrence Berkeley Laboratory, 1971, Internal Report.

31. D. Brown et al, Phys. Rev. Lett. 19, 664 (1967).

32. $\pi^+ n \to \omega^0 p$: 4.19 GeV/c A. S. Abrams, B. Eisenstein, H. Gordon, Phys. Rev. Lett. 23, 673 (1969).
5.1 GeV/c B. B. F.O. Collaboration, N.C. 65A, 637 (1970).
6.95 GeV/c J. A. J. Mathews et al., Phys. Rev. Lett. 26, 400 (1971).

32. $\pi^+ p \rightarrow \omega^o \Delta^{++}$: 2.3, 2.67 GeV/c (Ref. 35 below)

3.7 GeV/c G. S. Abrams, et al., Phys. Rev. Lett. 25, 617 (1970)

5.0 GeV/c (Ref. 37 below)

5.45 GeV/c (Ref. 38 below)

33. A Bandao, D. Schiff, and J. Tran Thanh Van, Orsay preprint, June 1971.

34. J. A. J. Mathews and I. O. Muen, University of Toronto preprint.

35. W. Ko, D. Grether, G. Gidal (to be published). W. Ko, Thesis, 19 1.

36. G. S. Abrams and U. Maor, Phys. Rev. Lett. 25, 615 (1970).

37. C. L. Pols et al., Nucl. Phys. B25, 109 (1970).

38. I. J. Bloodworth, W. C. Jackson, J. D. Prentice, T. S. Yoon, $\Delta^{++}\rho^o$ and $\Delta^{++}\omega^o$ Final States at 5.45 GeV/c - paper submitted to 1971 Annual Meeting of the Division of Particles and Fields.

Table I. SUMMARY

ρ Trajectory

$\alpha_{eff} = 0.57 + .91\ t$

NWSZ dip seen in both $\pi^- p \to \pi^o n$ and $\pi^+ p \to \pi^o \Delta^{++}$ near $t = -0.6$

A_2 Trajectory

$\alpha_{eff} = .34 + .35\ t$	$\pi^- p \to \eta^o n$
$\alpha_{eff} = .43 + .64\ t$	$\pi^- p \to \eta^o n$ $(4 < P_{Lab} < 20$ GeV/c)
$\alpha_{eff} = .87 + 1.75\ t$	$\pi^+ p \to \eta^o \Delta^{++}$
$\alpha = .58 + 1.01\ t$	$\pi^+ p \to \eta^o \Delta^{++}$ (K & M Amplitude Fit)

NWSZ dip near $t = -1.5$ seen in both $\pi^- p \to \eta^o n$ and $\pi^+ p \to \eta^o \Delta^{++}$

P' Trajectory

$\alpha_{eff} = .55 + .9\ t$	(Barger and Phillips)

Dips in $I_t = 0$ cross section near $t = -3$ and $t = -5$

ω^o Trajectory

$\alpha = .4 + t$	$\pi N \to \rho N$
$\alpha(0) = 0.47 \pm 0.09$	$K_L^o p \to K_S^o p$
$\alpha(0) = 0.38 \pm 0.04$	σ_T

NWSZ dip near $t = -0.4$ seen in $I_t = 0$ cross section at 2.7 GeV/c

B Trajectory

$\alpha = 0.12 + 0.6\ t$	Dip position + B mass Fits $\pi^+ n \to \omega^o p$
$\alpha = -0.2 + 0.8\ t$	Fits $\pi^+ n \to \omega^o p$
$\alpha_{eff} = (.15 \pm .12) + (.62 \pm .23)\ t$	$\pi^+ p \to \omega^o \Delta^{++}$

π-B Exchange Degeneracy Model

$\alpha \approx 1.12\ t$	at 3.7 GeV/c
$\alpha \approx 1.17\ t$	at 5.0 GeV/c
$\alpha \approx 1.34\ t$	at 5.45 GeV/c

Fits $\pi^+ p \to \rho^o \Delta^{++}$, $\omega^o \Delta^{++}$; $K^+ p \to K^{*o} \Delta^{++}$

Nature of dip near $t = -0.2$ in doubt.

Figure Captions

Fig. 1. Effective Regge trajectory for $\pi^- p \rightarrow \pi^o n$ ($P_{Lab} \leq 5$ GeV/c). Reference 4.

Fig. 2. Differential cross section, $d\sigma/dt$, for $\pi^- p \rightarrow \pi^o n$. Reference 6.

Fig. 3. Differential cross section, $d\sigma/dt$, for $\pi^+ p \rightarrow \pi^o \Delta^{++}$. Reference 7.

Fig. 4. Effective Regge trajectory for $\pi^+ p \rightarrow \eta^o \Delta^{++}$. Reference 9.

Fig. 5. Partial wave coefficients for reaction $\pi^+ p \rightarrow \eta^o \Delta^{++}$. Solid curves are Regge amplitudes from best fit between 2.3 and 8 GeV/c.

Fig. 6. Differential cross section, $d\sigma/dt$, for $\pi^+ p \rightarrow \eta^o \Delta^{++}$ before (a) and after (b) background subtraction. The solid curve is the Regge amplitude fit of Krammer and Maor. Reference 9.

Fig. 7. Differential cross section, $d\sigma/dt$, for $\pi^- p \rightarrow \eta^o n$. Squares are the data of Reference 12 and crosses are the data of Reference 13.

Fig. 8. The position of the minima in the differential cross section for $\pi^- p \rightarrow \eta^o n$. Reference 14.

Fig. 9. Model independent s-channel helicity amplitudes and phases for the $I_t = 1$ component of the πN scattering from Reference 15. Solid curves are the Regge pole fits of Reference 16.

Fig. 10. Separate $I_t = 0$ and $I_t = 1$ differential πN cross sections at 4 and 5 GeV/c. Reference 4.

Fig. 11. Differential cross section for $\pi^+ p \rightarrow \rho^+ p$ at 2.67 GeV/c. Reference 17.

Fig. 12. $X(t) = \frac{1}{2}\left\{\frac{d\sigma}{dt}(\pi^+p \to \rho^+p) + \frac{d\sigma}{dt}(\pi^-p \to \rho^-p) - \frac{d\sigma}{dt}(\pi^-p \to \rho^0 n)\right\}$ at 2.7 GeV/c. Reference 17.

Fig. 13. Chew-Frautschi plot of current data on ω^0 trajectory.

Fig. 14. The angular distribution of the phase between the $I_t = 0$ and $I_t = 1$ exchanges in $\pi N \to \rho N$ at 2.7 GeV/c. Reference 17.

Fig. 15. Density matrix element, ρ_{00}^H, in helicity frame and $\rho_{00}^H\, d\sigma/dt$ for $\pi^+p \to \rho^+p$ at 2.67 GeV/c. Reference 17.

Fig. 16. Angular distributions for $\pi^\pm p \to A_2^\pm p$ with $A_2^\pm \to K_S^0 K^\pm$. Reference 25.

Fig. 17. Angular distributions for $\pi^\pm p \to A_2^\pm p$ with $A_2^\pm \to \pi^\pm \eta^0$. Reference 25.

Fig. 18. Compilation of density matrix element, ρ_{00} for $\pi^+n \to \omega^0 p$ and $\pi^+p \to \omega^0\Delta^{++}$. Reference 32.

Fig. 19. Differential cross section, $d\sigma/dt$, for $\pi^+n \to \omega^0 p$. Solid curve is best fit of Reference 33.

Fig. 20. The (s-u) dependence of helicity non-flip unnatural parity exchange contribution to $\pi^+p \to \omega^0\Delta^{++}$. Reference 35.

Fig. 21. Effective trajectory for unnatural parity exchange contribution to $\pi^+p \to \omega^0\Delta^{++}$. Reference 35.

Fig. 22. The unnatural parity exchange contribution, $\rho_{00}\, d\sigma/dt$, to the reactions $\pi^+p \to \omega^0\Delta^{++}$, $\pi^+p \to \rho^0\Delta^{++}$ at 2.7, 5.0, and 5.45 GeV/c. The solid curves are the best fits to the model of Abrams and Maor. References 36, 37, 38.

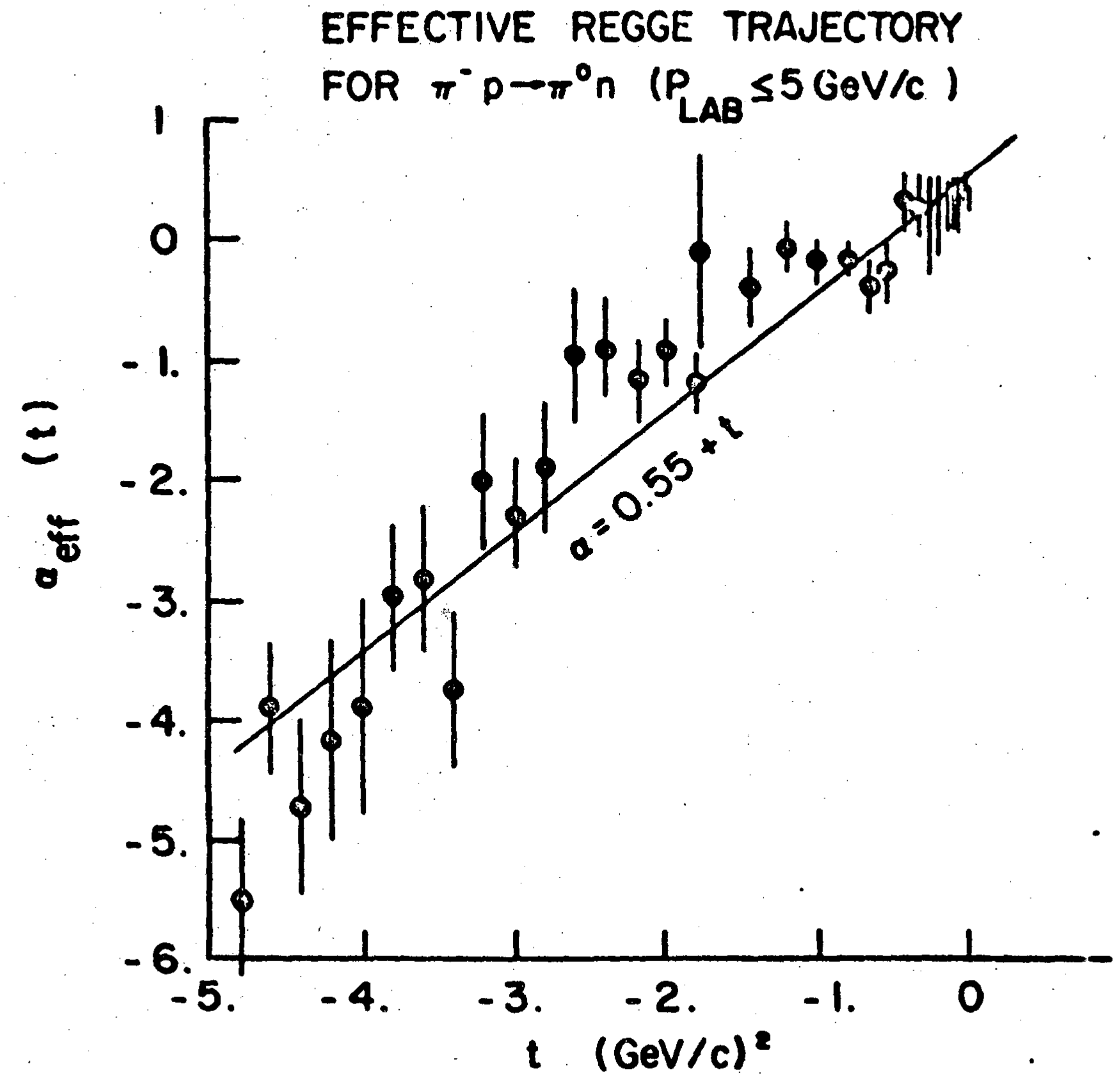
EFFECTIVE REGGE TRAJECTORY
FOR $\pi^- p \to \pi^0 n$ ($P_{LAB} \leq 5$ GeV/c)
$\alpha = 0.55 + t$
α_{eff} (t)
1
0
-1.
-2.
-3.
-4.
-5.
-6.
-5.
-4.
-3.
-2.
-1.
0
t (GeV/c)²

Fig. 1

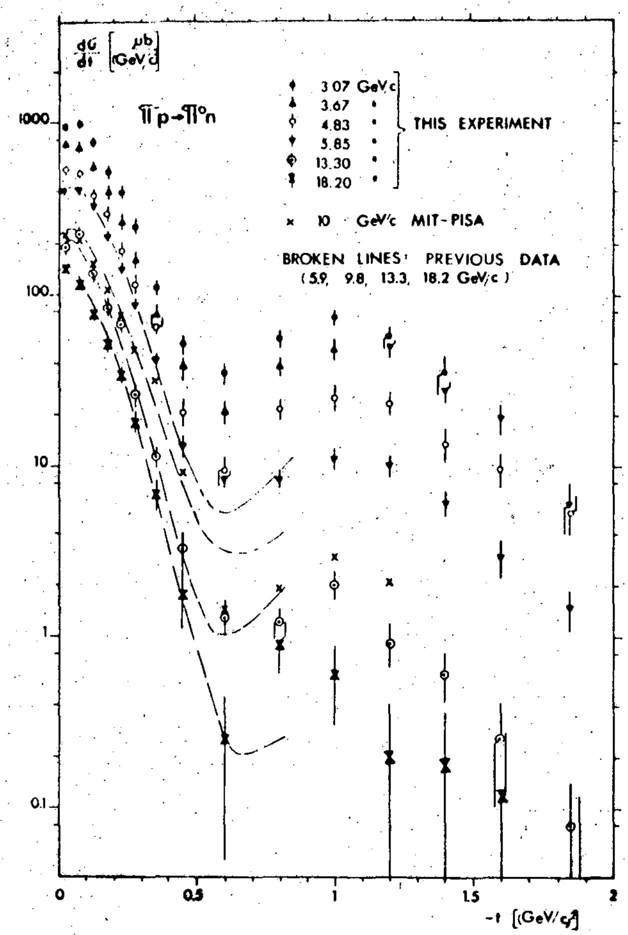

dσ/dt [μb/(GeV/c)²]
π⁻p→π⁰n
3.07 GeV/c
3.67 "
4.83 "
5.85 "
13.30 "
18.20 "
THIS EXPERIMENT
x 10 GeV/c MIT-PISA
BROKEN LINES: PREVIOUS DATA
(5.9, 9.8, 13.3, 18.2 GeV/c)
1000
100
10
1
0.1
0
0.5
1
1.5
2
-t [(GeV/c)²]

Fig. 2

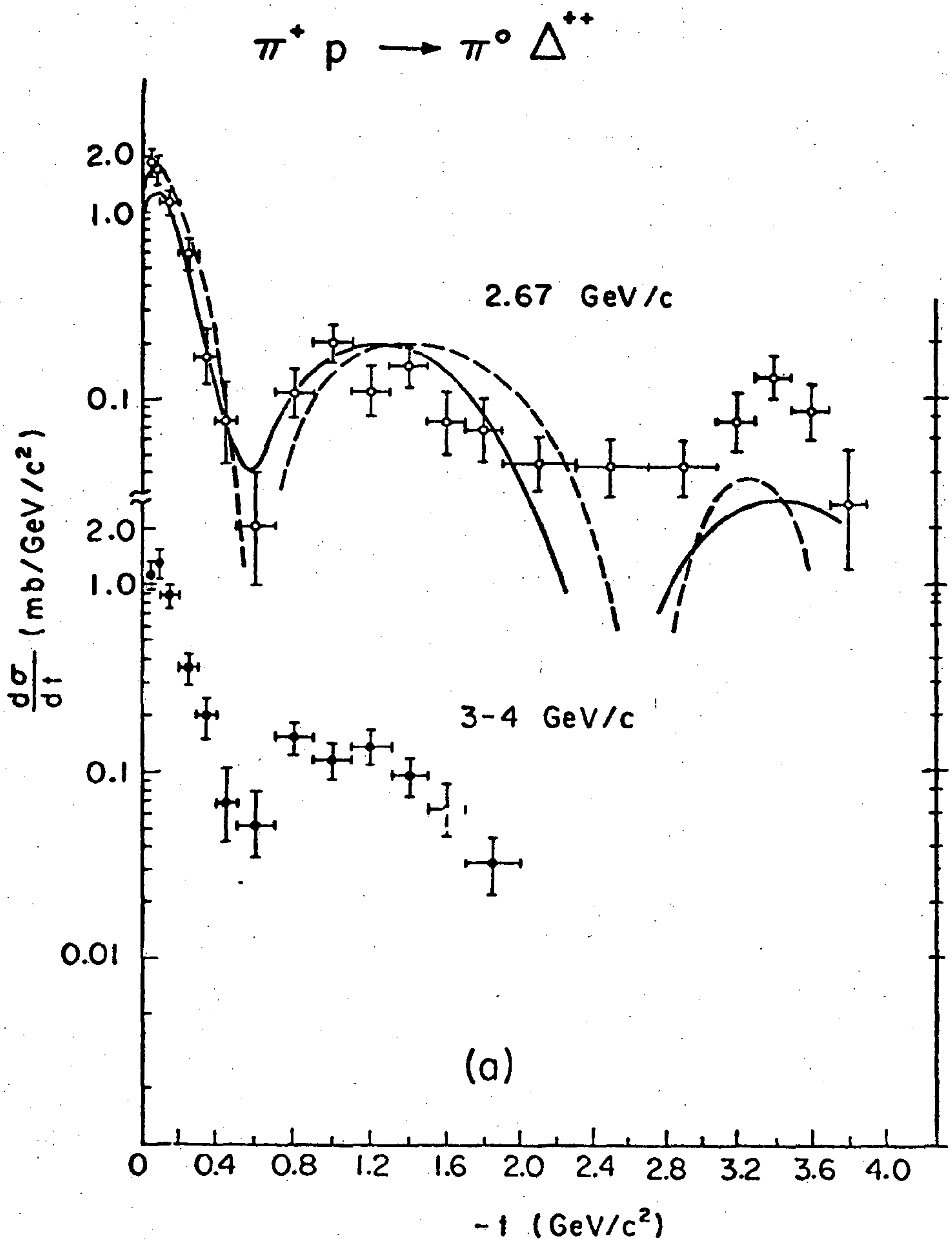

$\pi^+ p \rightarrow \pi^0 \Delta^{++}$
2.67 GeV/c
3-4 GeV/c
$\frac{d\sigma}{dt}$ (mb/GeV/c^2)
2.0
1.0
0.1
0.01
0
0.4
0.8
1.2
1.6
2.0
2.4
2.8
3.2
3.6
4.0
$-t$ (GeV/c^2)
(a)

Fig. 3

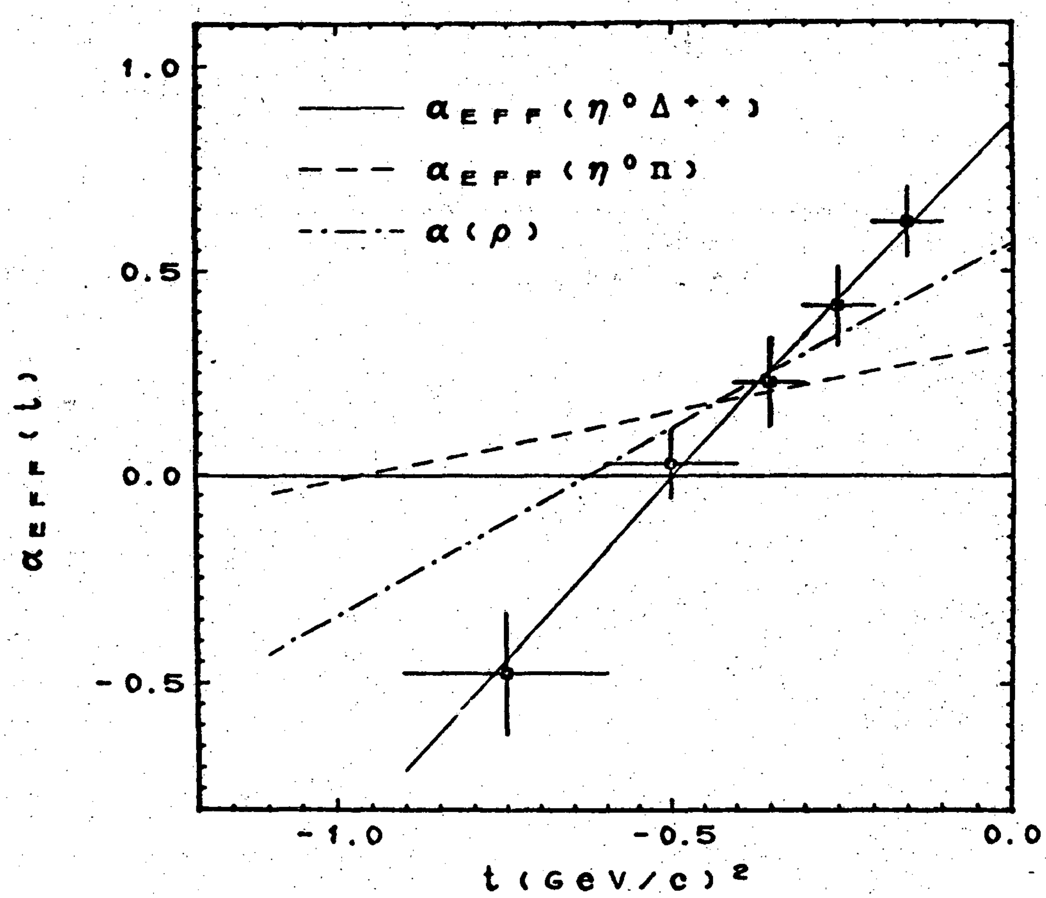

XBL 7012-7413

Fig. 4

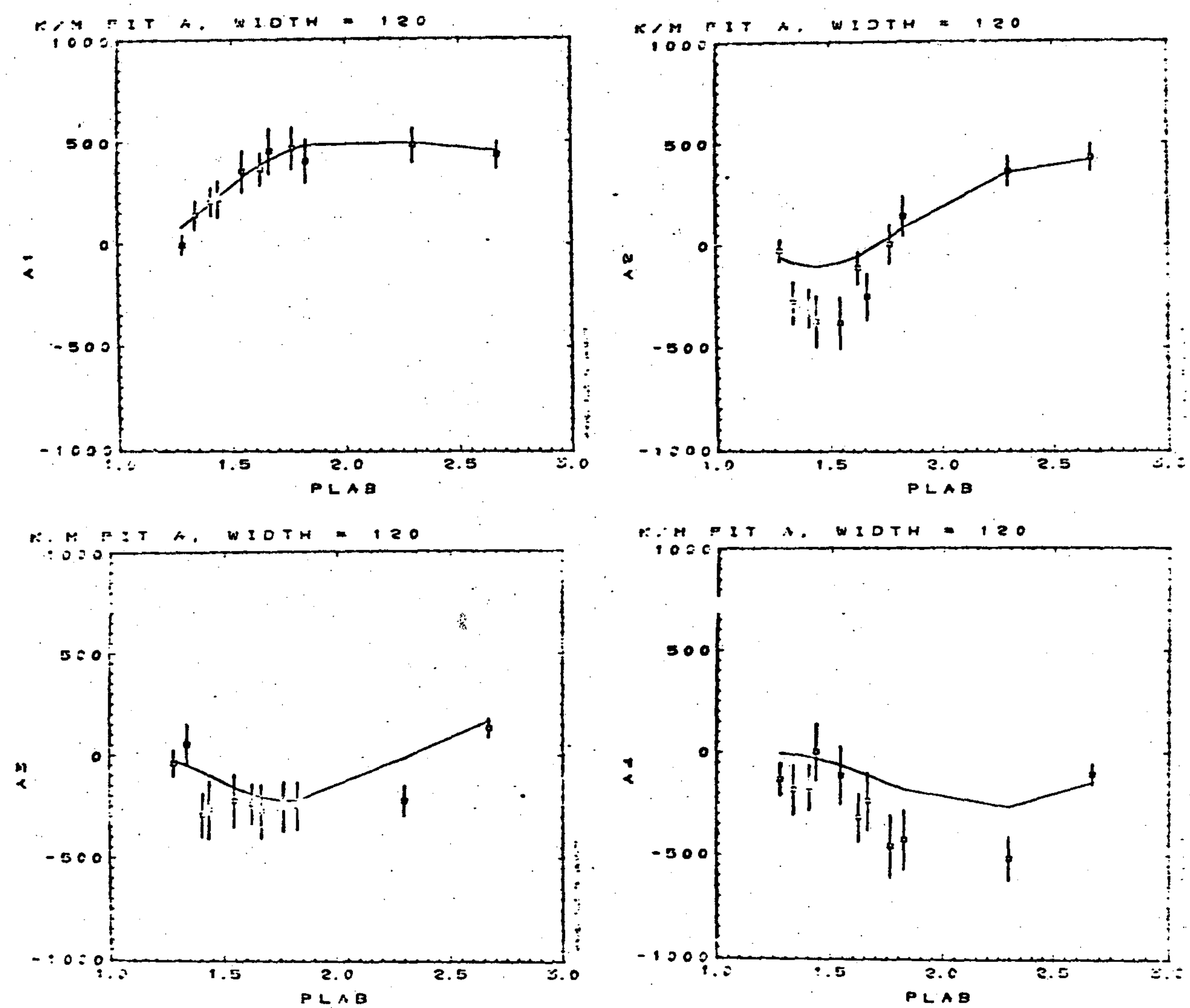
K/M FIT A, WIDTH = 120
1000
500
0
-500
-1000
1.0
1.5
2.0
2.5
3.0
A1
PLAB
K/M FIT A, WIDTH = 120
A2
PLAB
K/M FIT A, WIDTH = 120
A3
PLAB
K/M FIT A, WIDTH = 120
A4
PLAB

Fig. 5

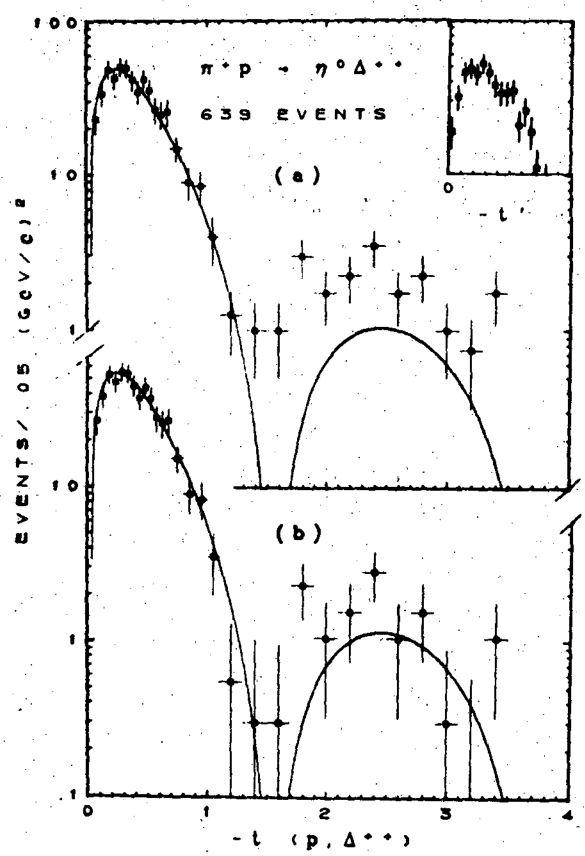

Fig. 6

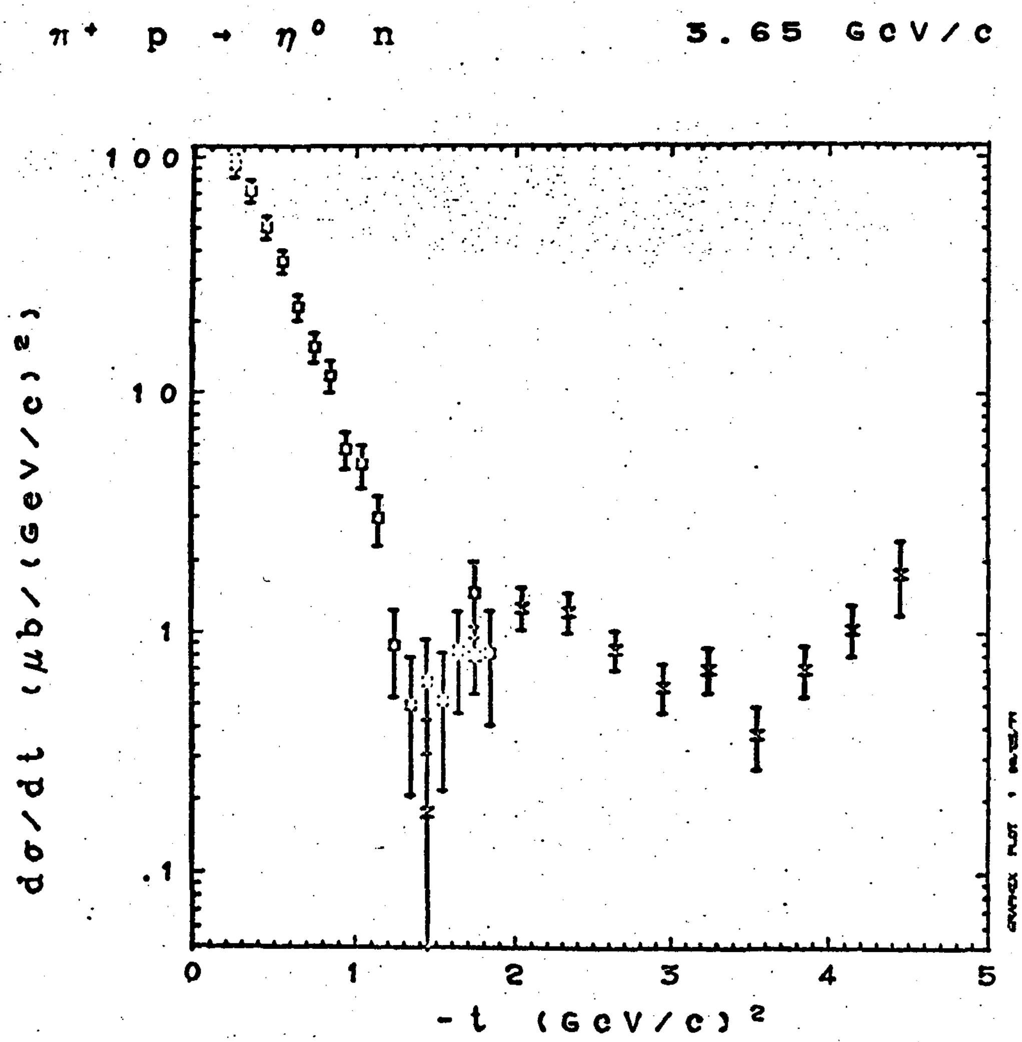

Fig. 7

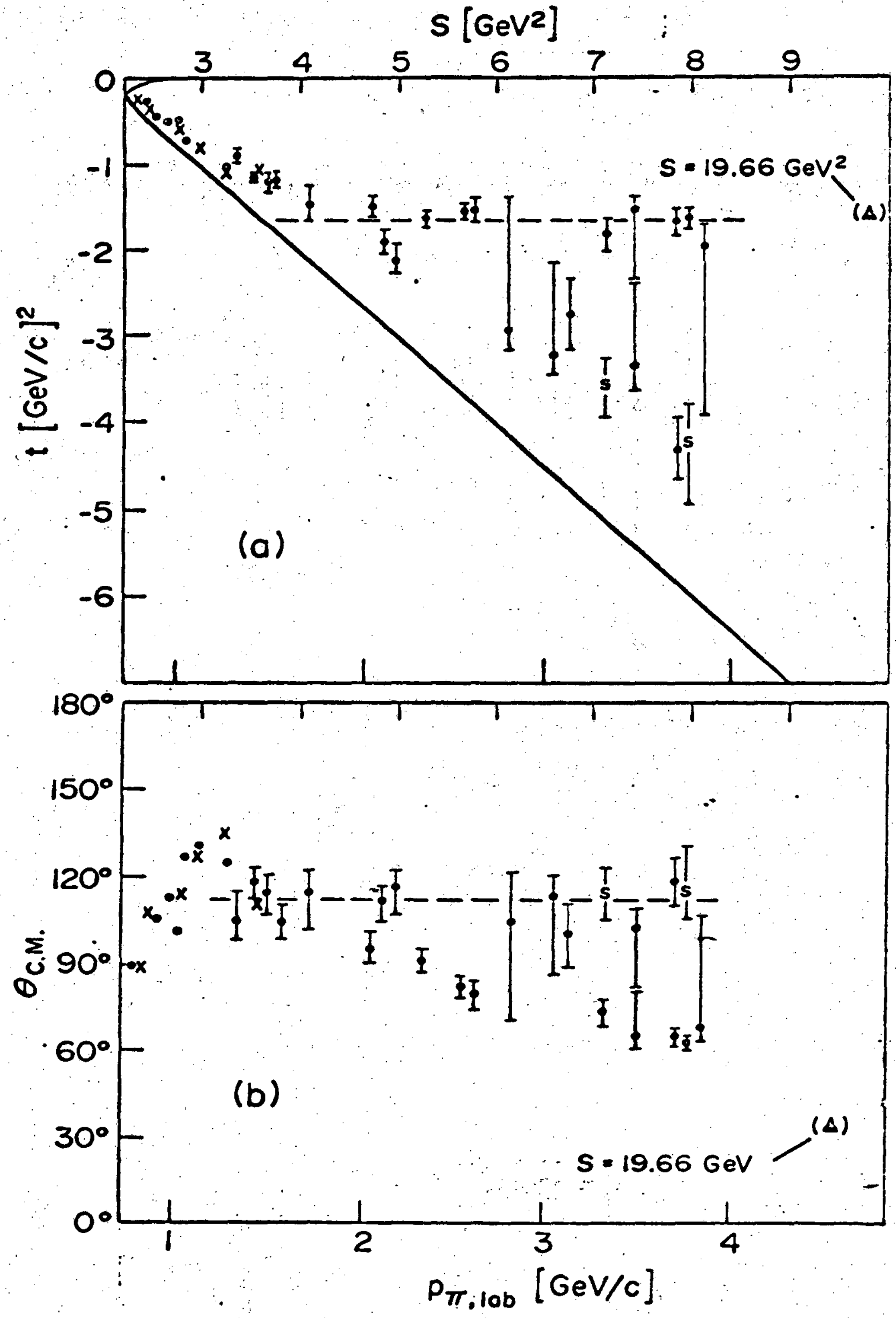
S [GeV²]
3
4
5
6
7
8
9
0
-1
-2
-3
-4
-5
-6
t [GeV/c]²
S = 19.66 GeV²
(Δ)
s
s
(a)
180°
150°
120°
90°
60°
30°
0°
θ C.M.
s
s
(b)
S = 19.66 GeV
(Δ)
1
2
3
4
p π, lab [GeV/c]

Fig. 8

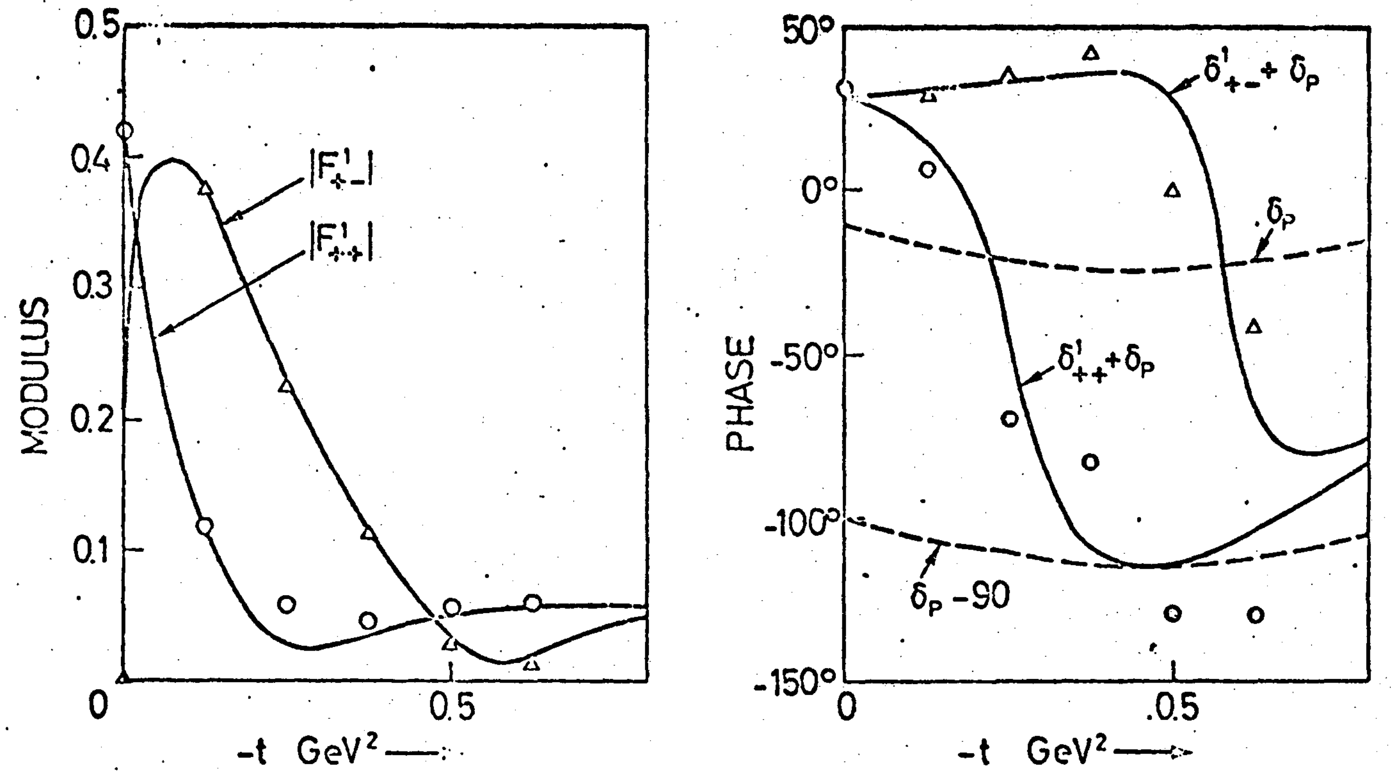

πN s channel helicity amplitudes
$I_t=1$ 6 GeV/c

Fig. 9

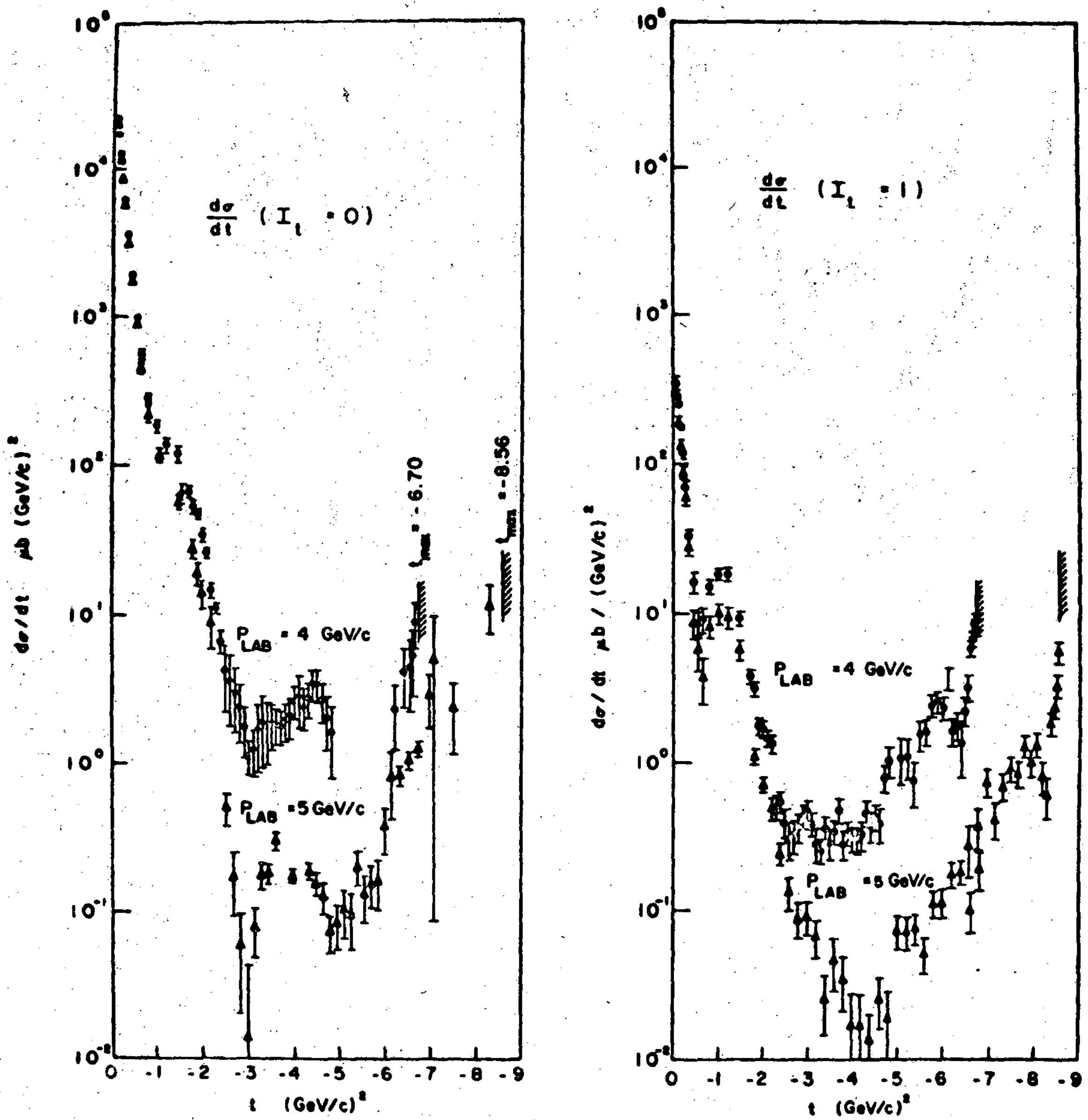
dσ/dt (I_t = 0)
dσ/dt μb (GeV/c)²
P_LAB = 4 GeV/c
P_LAB = 5 GeV/c
t_max = -6.70
t_max = -8.56
t (GeV/c)²
dσ/dt (I_t = 1)
dσ/dt μb / (GeV/c)²
P_LAB = 4 GeV/c
P_LAB = 5 GeV/c
t (GeV/c)²

Fig. 10

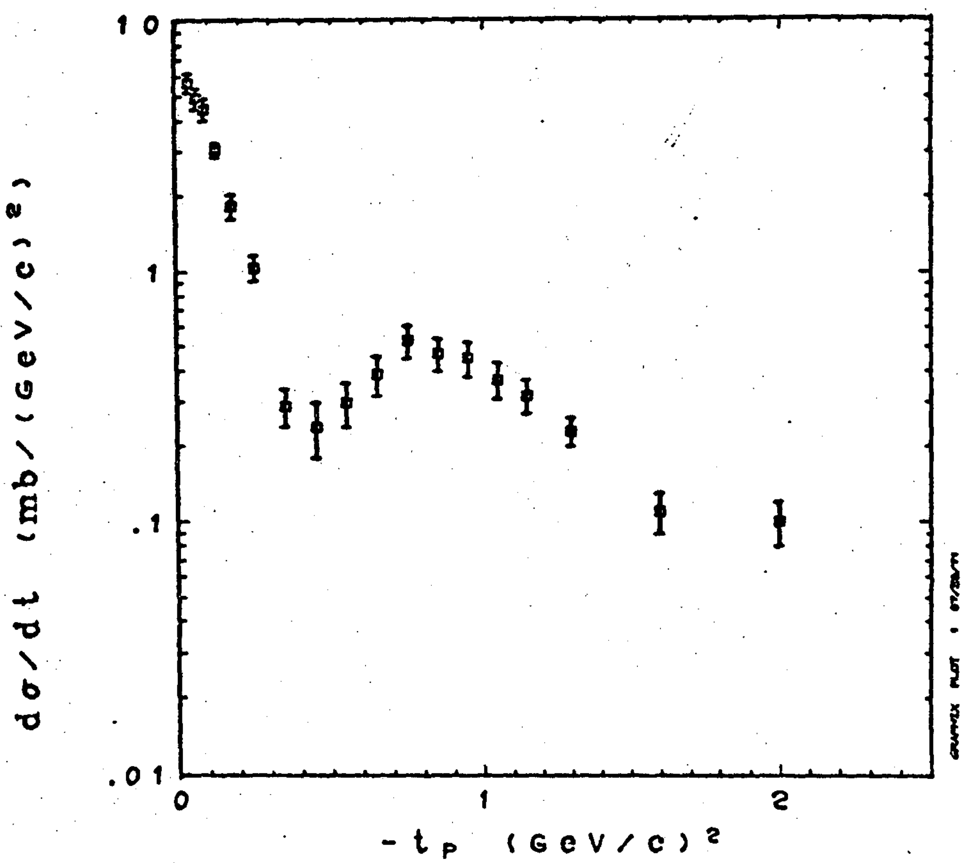

Fig. II

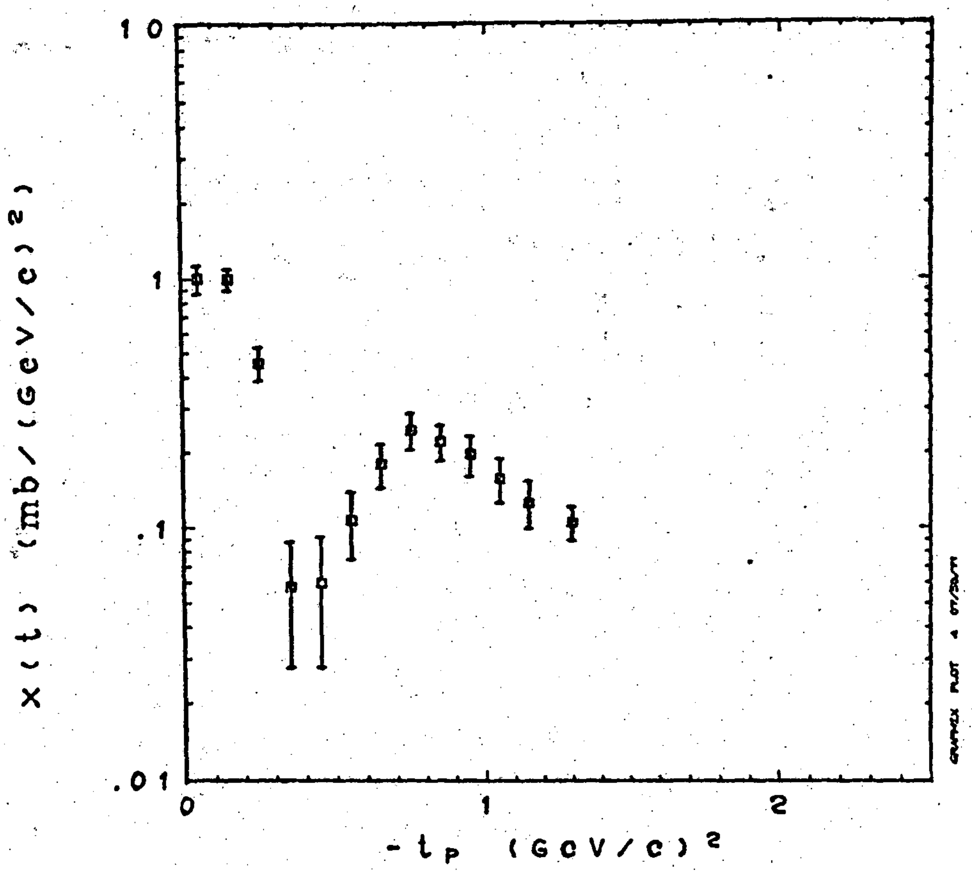

Fig. 12

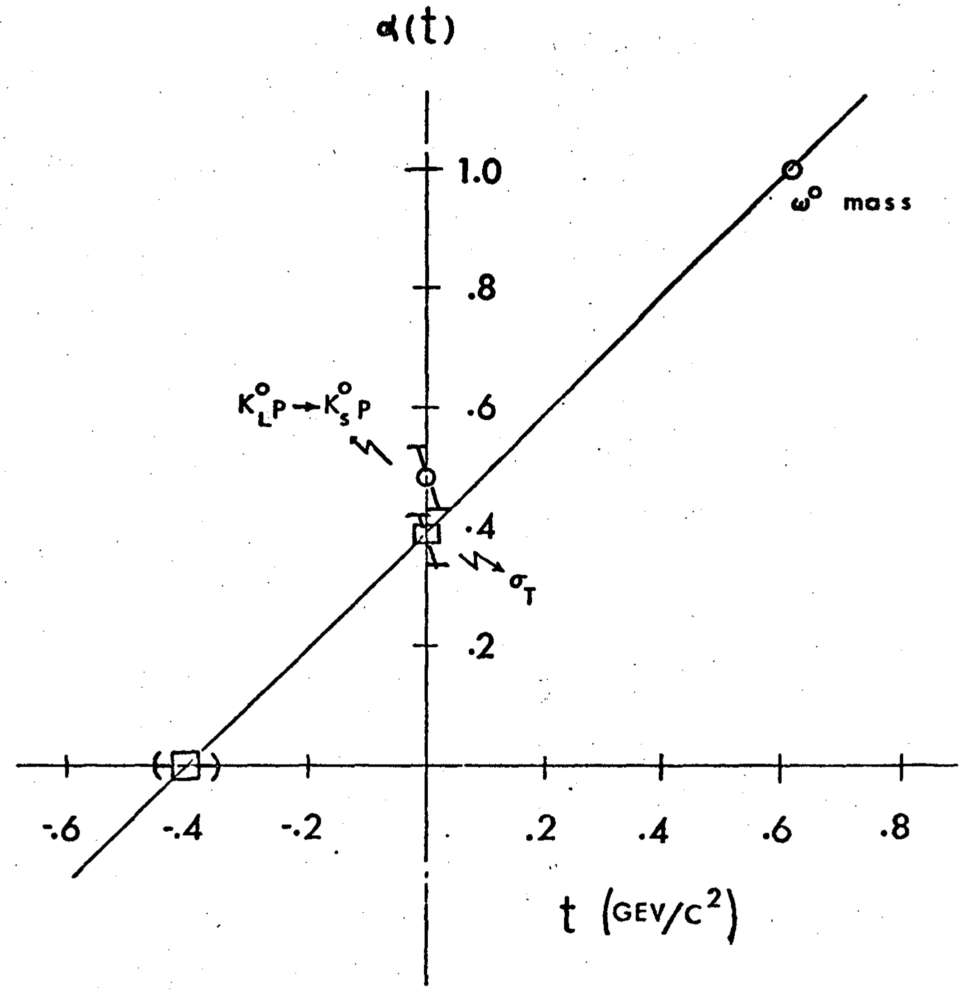

α(t)
1.0
.8
.6
.4
.2
ω^0 mass
$K_L^0 P \rightarrow K_s^0 P$
σ_T
-.6
-.4
-.2
.2
.4
.6
.8
t (GEV/c²)

Fig. 13

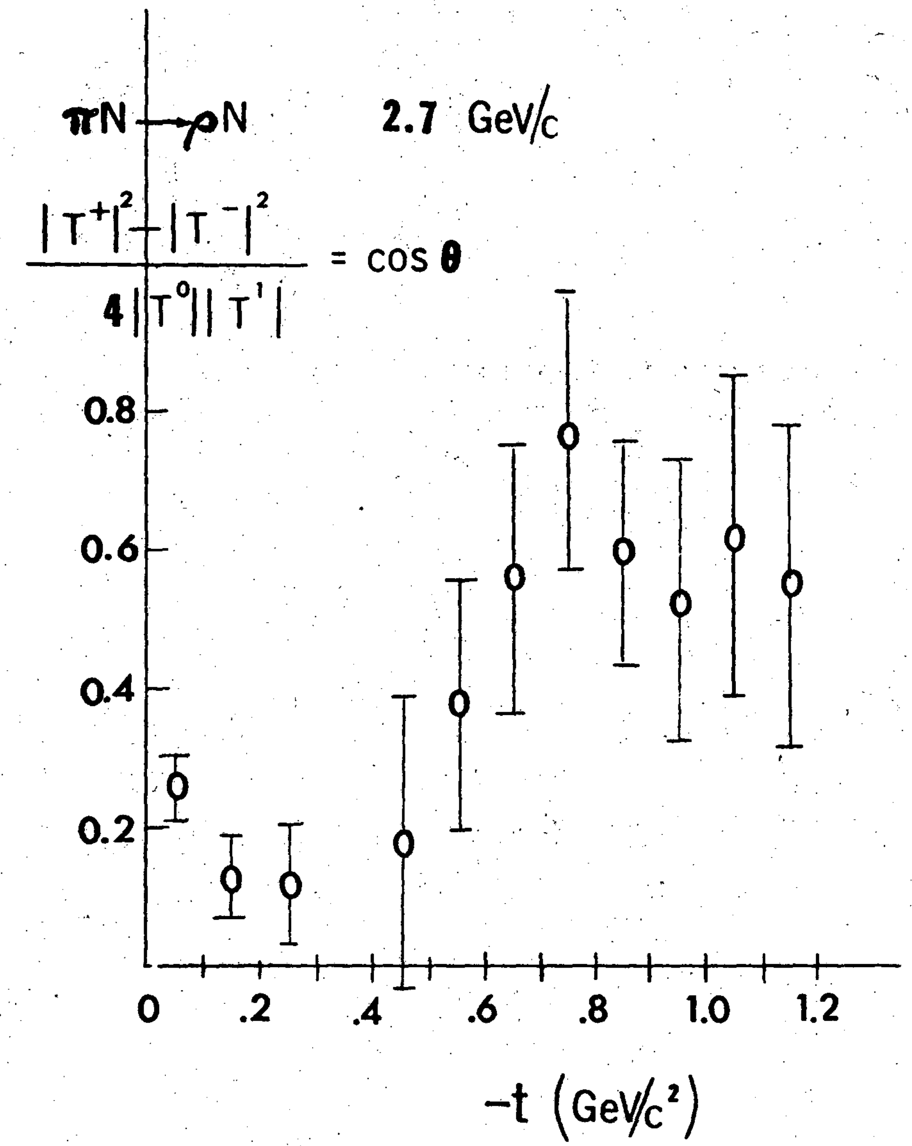

πN → ρN
2.7 GeV/c
$\frac{|T^+|^2 - |T^-|^2}{4|T^0||T^1|} = \cos\theta$
0.8
0.6
0.4
0.2
0
.2
.4
.6
.8
1.0
1.2
-t (GeV/c²)

Fig. 14

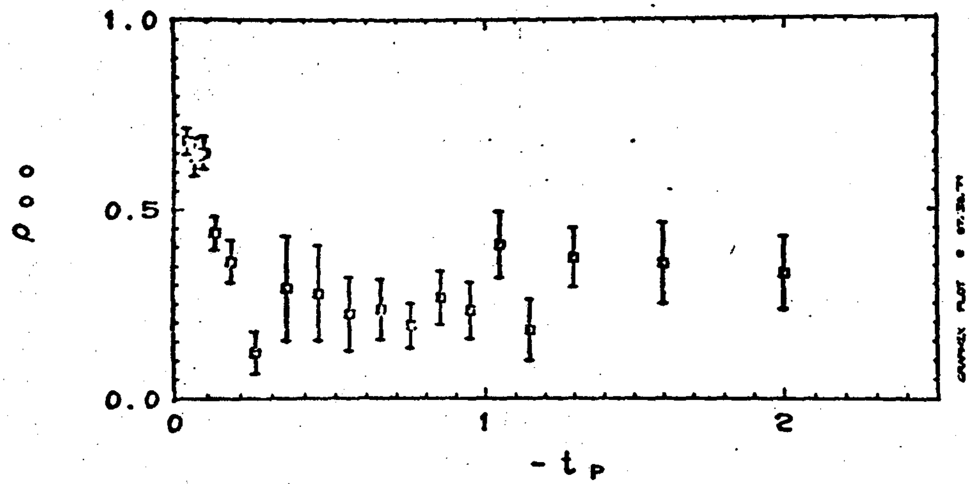

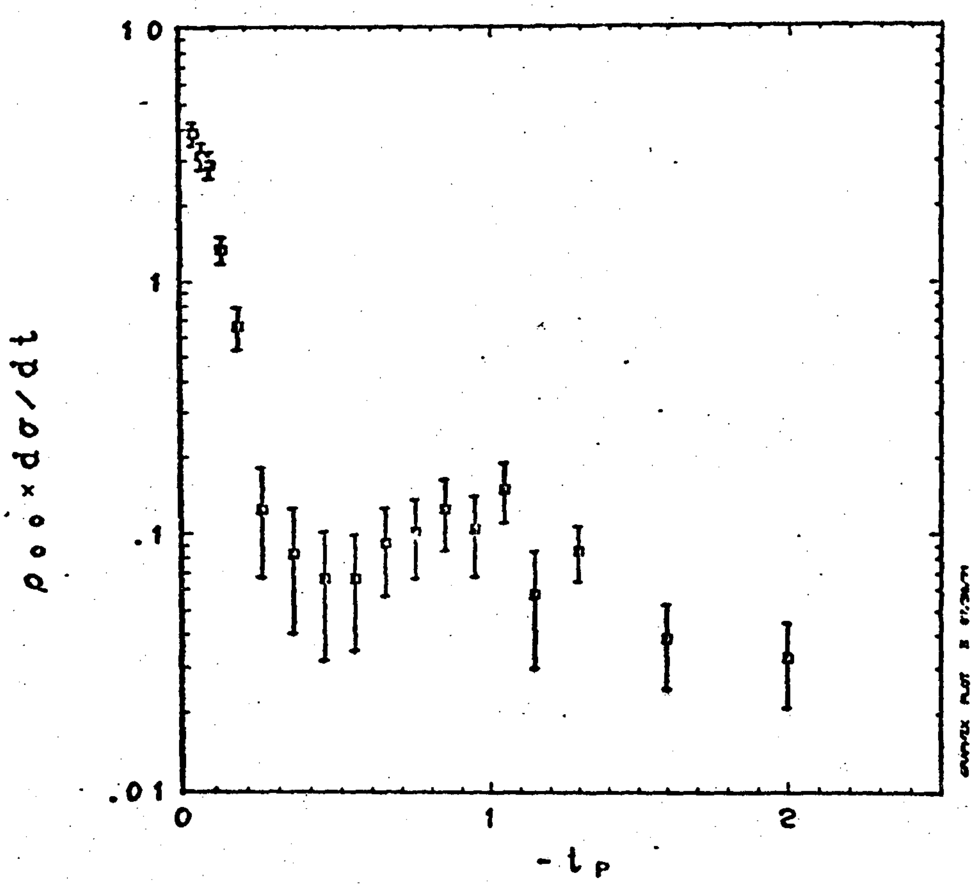

Fig. 15

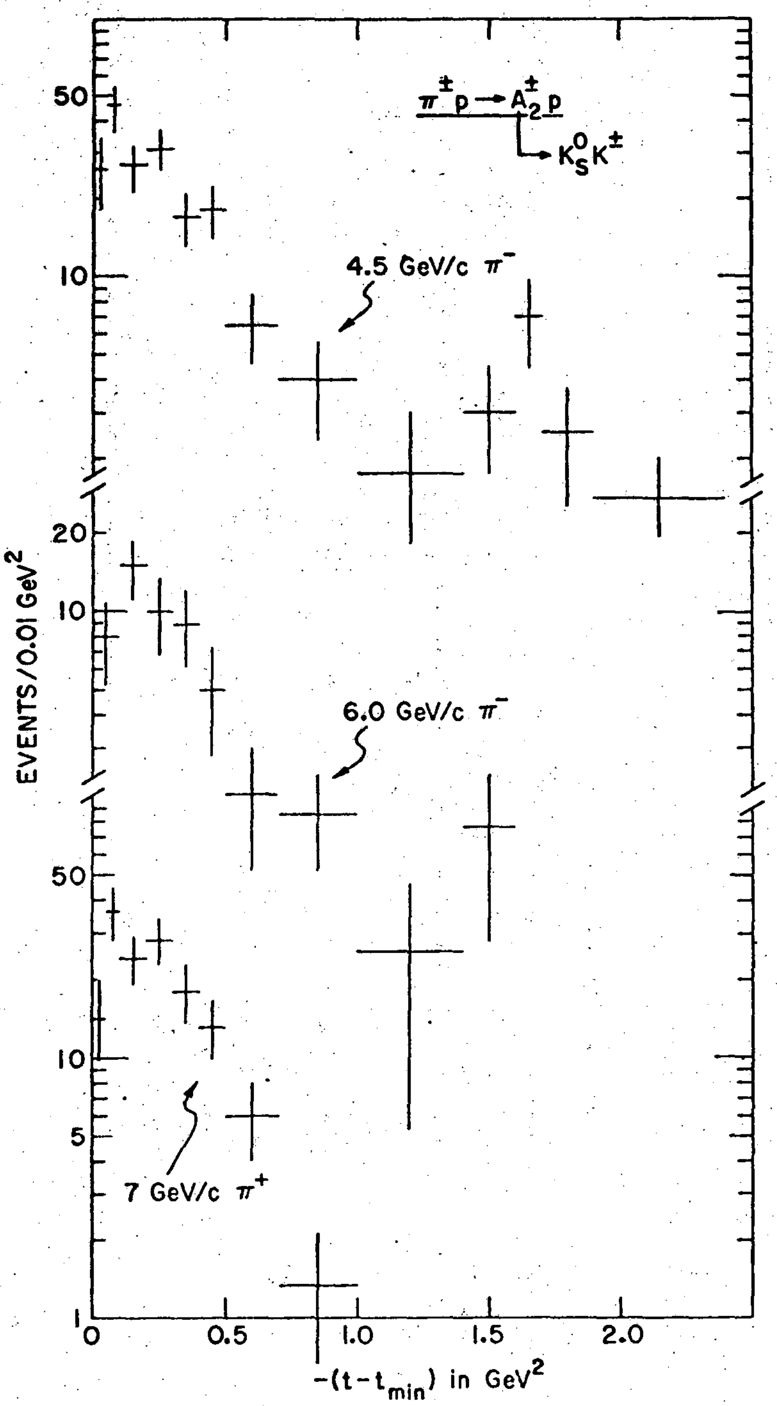

$\pi^{\pm}p \rightarrow A_2^{\pm}p$
$\hookrightarrow K_S^0 K^{\pm}$
4.5 GeV/c π^-
6.0 GeV/c π^-
7 GeV/c π^+
EVENTS/0.01 GeV^2
50
10
20
10
50
10
5
1
0
0.5
1.0
1.5
2.0
$-(t-t_{min})$ in GeV^2

Fig. 16

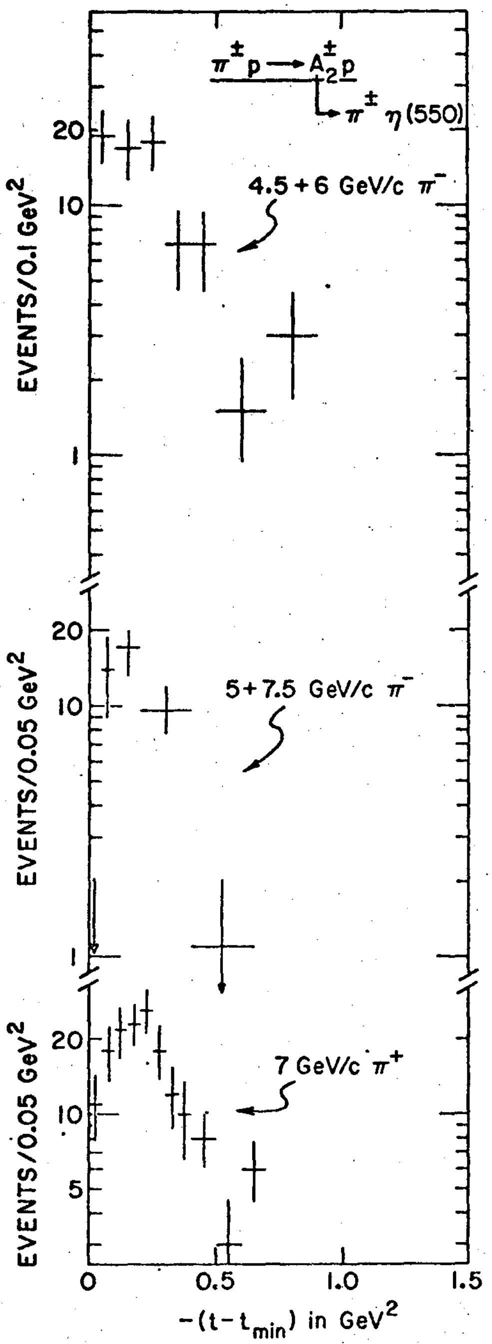

$\pi^\pm p \to A_2^\pm p$
$\hookrightarrow \pi^\pm \eta(550)$
4.5 + 6 GeV/c π^-
5 + 7.5 GeV/c π^-
7 GeV/c π^+
EVENTS/0.1 GeV^2
EVENTS/0.05 GeV^2
EVENTS/0.05 GeV^2
20
10
1
20
10
1
20
10
5
0
0.5
1.0
1.5
$-(t-t_{min})$ in GeV^2

Fig. 17

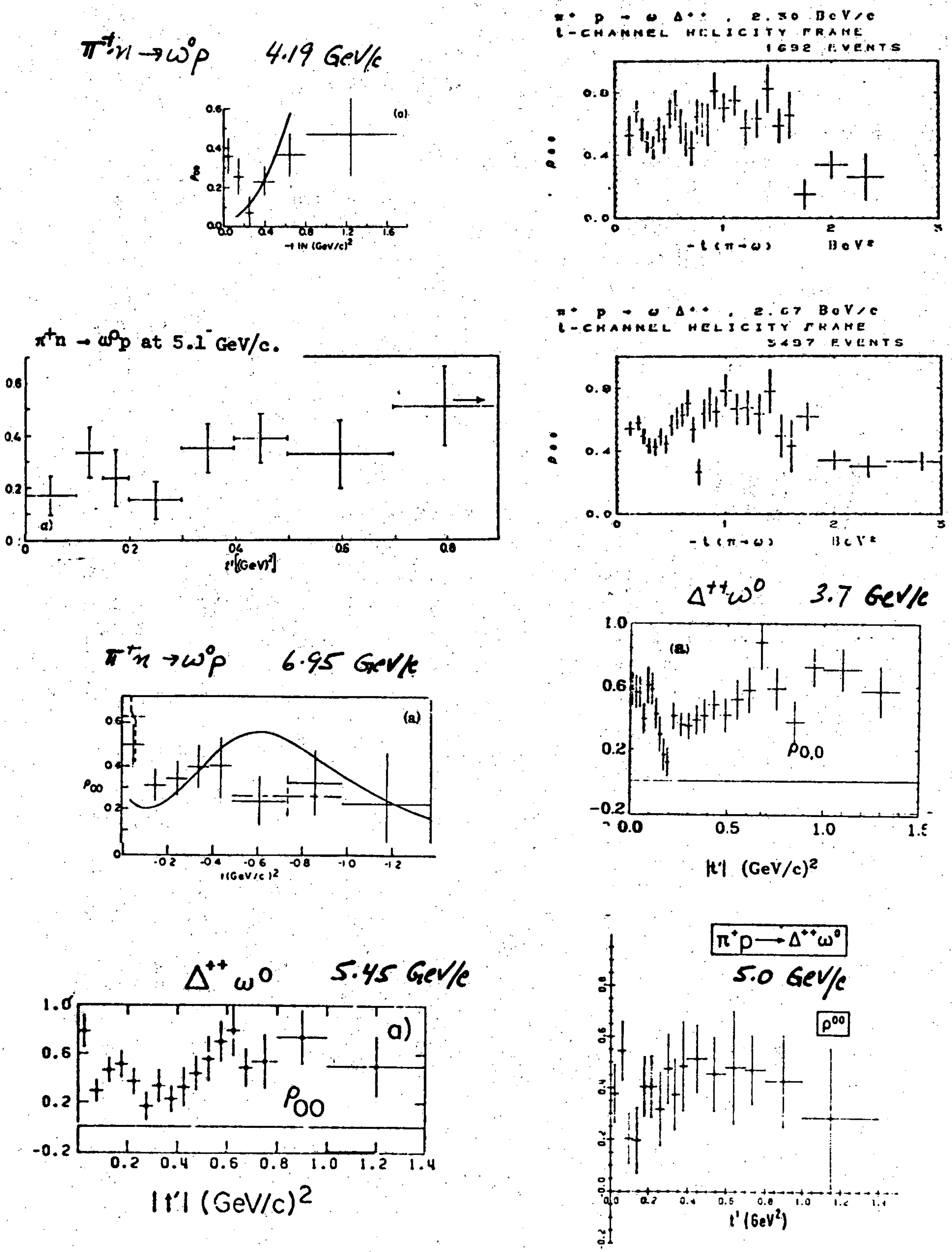
π⁺n → ω⁰p 4.19 GeV/c
-t IN (GeV/c)²
π⁺ p → ω Δ⁺⁺ , 2.30 BeV/c
t-CHANNEL HELICITY FRAME
1692 EVENTS
-t (π→ω) BeV²
π⁺n → ω⁰p at 5.1 GeV/c.
t'[GeV²]
π⁺ p → ω Δ⁺⁺ , 2.67 BeV/c
t-CHANNEL HELICITY FRAME
3497 EVENTS
-t (π→ω) BeV²
Δ⁺⁺ω⁰ 3.7 GeV/c
(a)
ρ0,0
|t'| (GeV/c)²
π⁺n → ω⁰p 6.95 GeV/c
(a)
ρ00
t (GeV/c)²
Δ⁺⁺ ω⁰ 5.45 GeV/c
a)
ρ00
|t'| (GeV/c)²
π⁺p → Δ⁺⁺ω⁰
5.0 GeV/c
ρ00
t' (GeV²)

Fig. 18

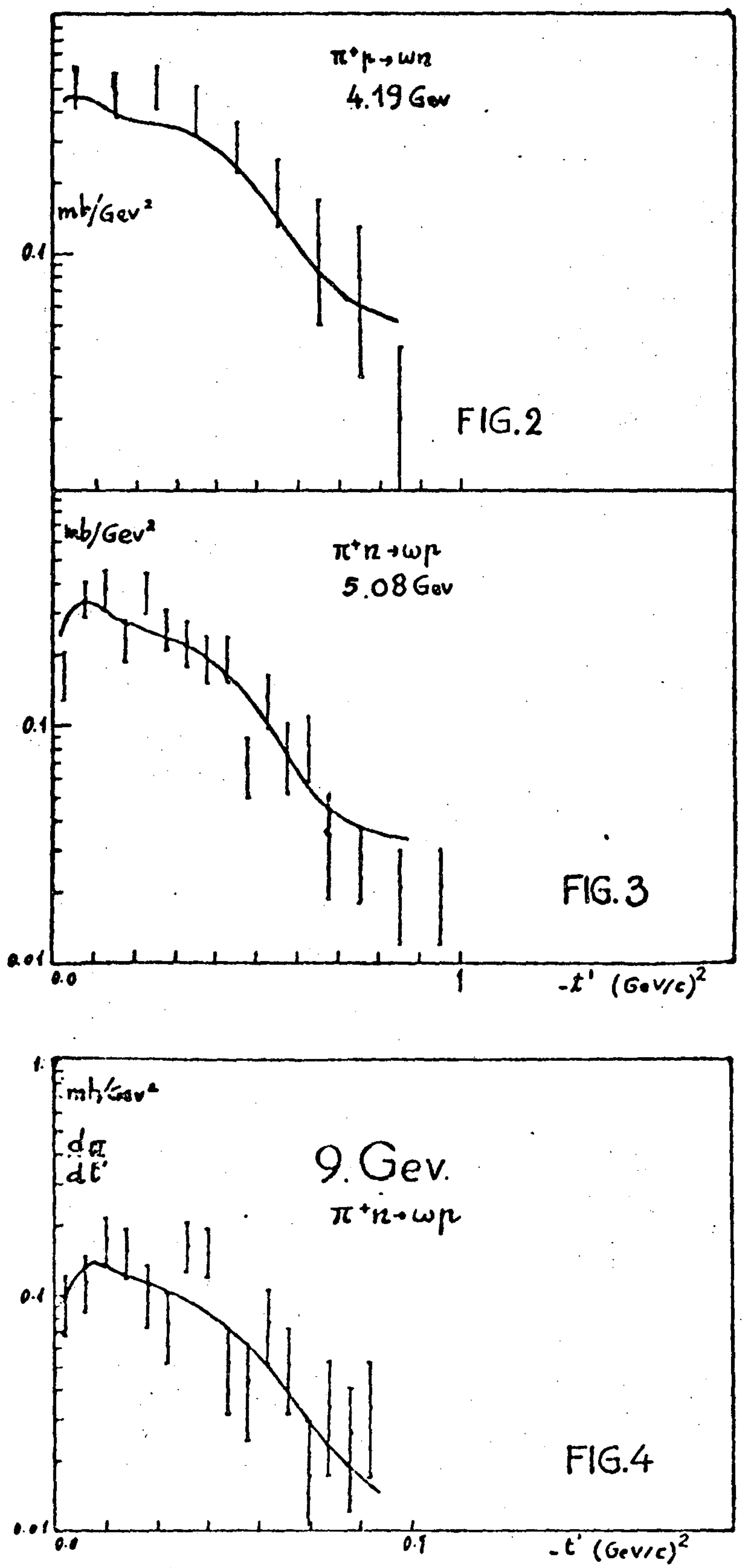

π⁺p→ωn
4.19 Gev
mb/Gev²
0.1
FIG.2
mb/Gev²
π⁺n→ωp
5.08 Gev
0.1
0.01
FIG.3
0.0
1
-t' (Gev/c)²
1.
mb/Gev²
dσ/dt'
9. Gev.
π⁺n→ωp
0.1
0.01
FIG.4
0.0
0.1
-t' (Gev/c)²

Fig. 19

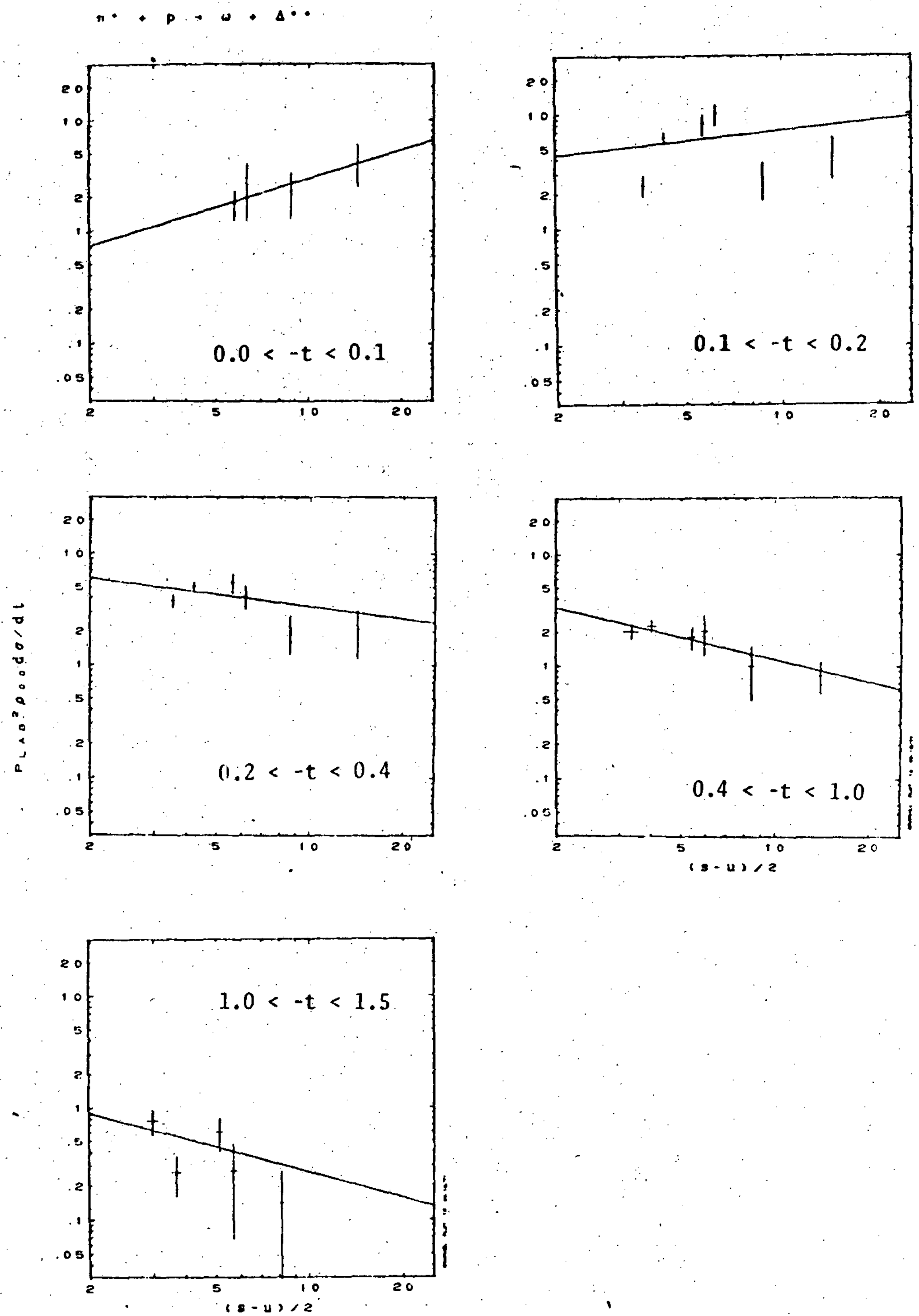

Fig. 20

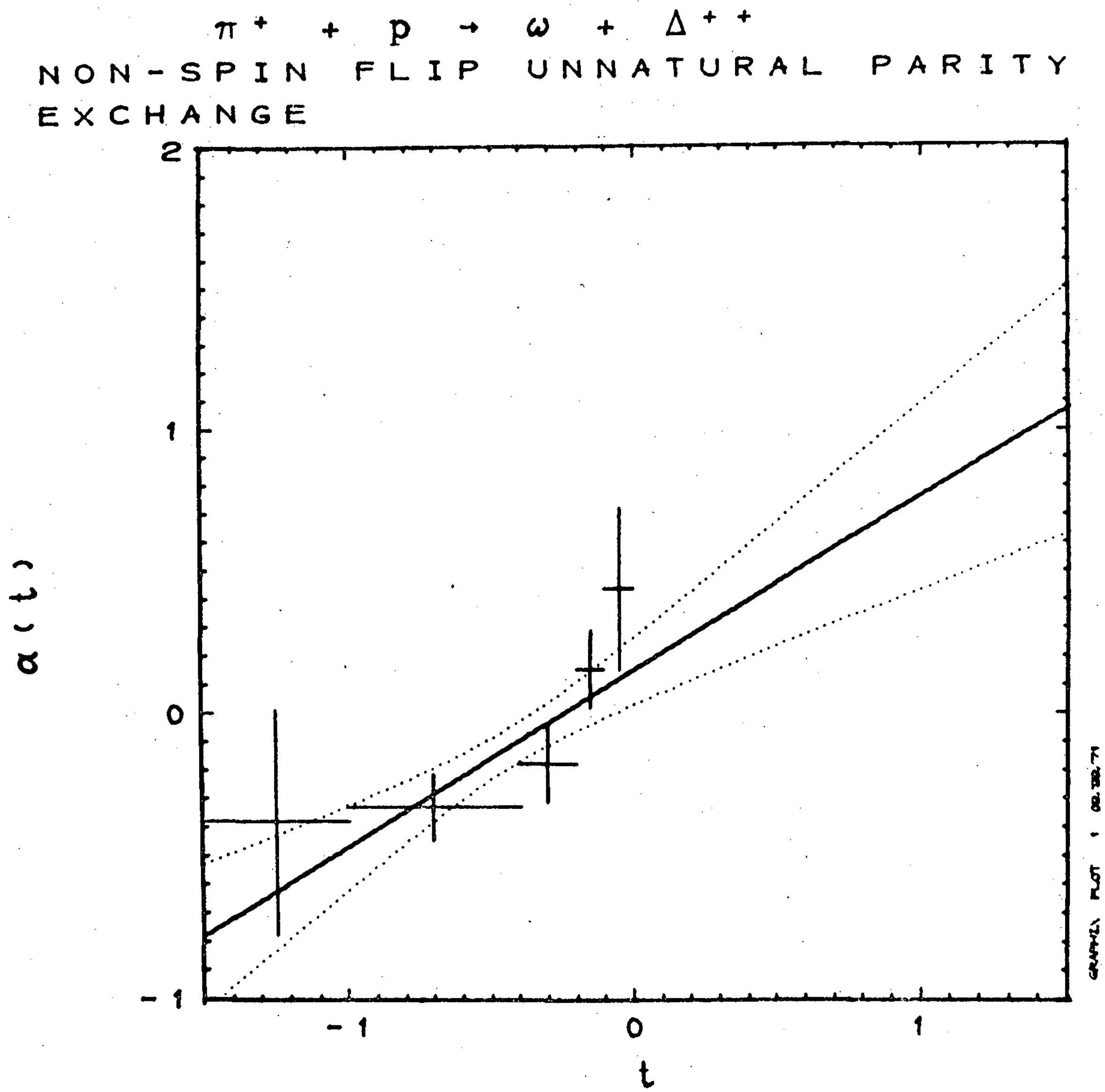

XBL 712-339

Fig. 21

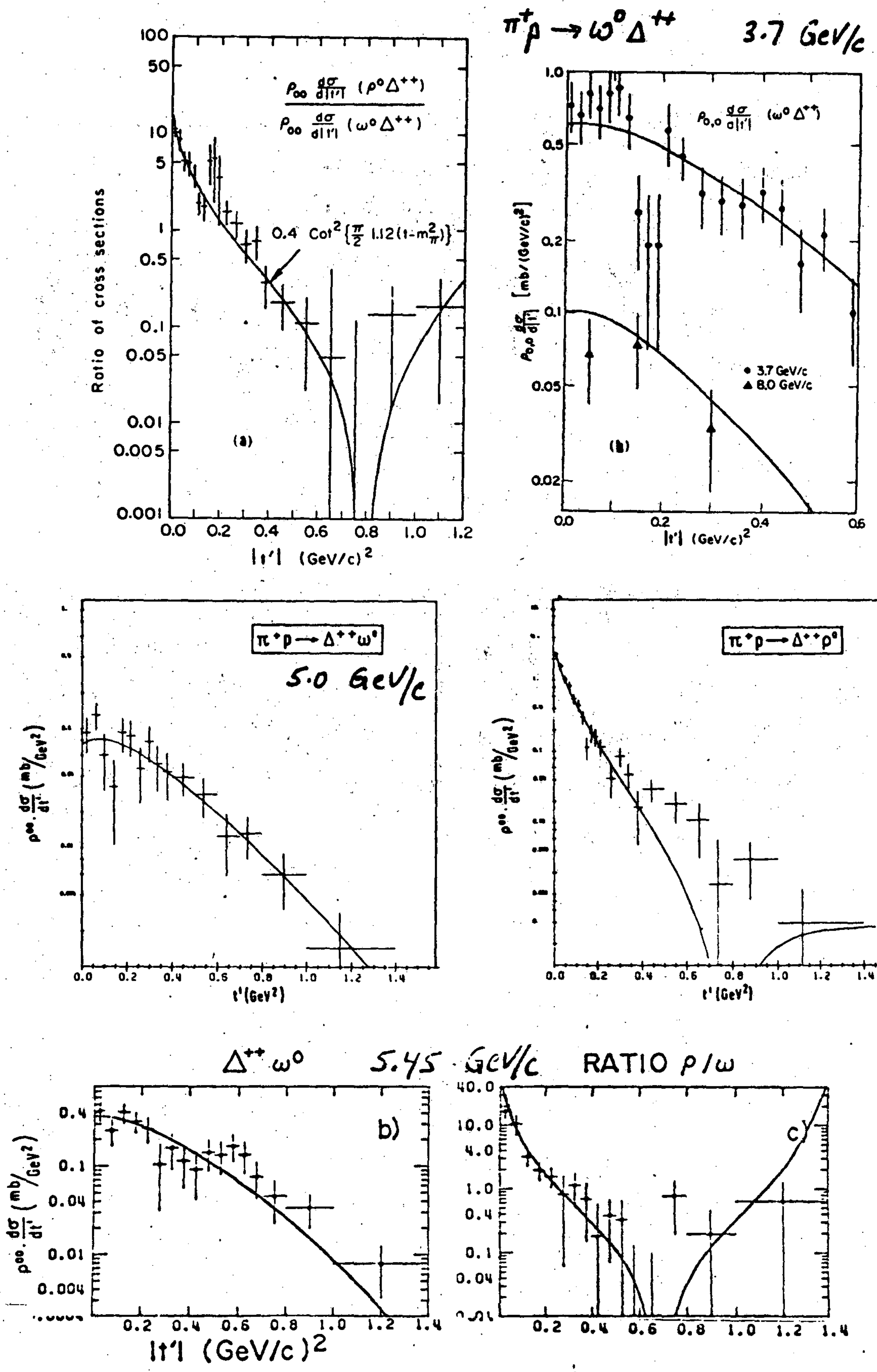

π⁺p → ω⁰Δ⁺⁺ 3.7 GeV/c
Ratio of cross sections
0.4 Cot²{π/2 1.12(t−m²π)}
(a)
|t'| (GeV/c)²
ρ0,0 dσ/d|t'| (ω⁰ Δ⁺⁺)
ρ0,0 dσ/d|t'| [mb/(GeV/c)²]
• 3.7 GeV/c
▲ 8.0 GeV/c
(b)
π⁺p → Δ⁺⁺ω⁰
5.0 GeV/c
ρ⁰⁰ · dσ/dt' (mb/GeV²)
t' (GeV²)
π⁺p → Δ⁺⁺ρ⁰
Δ⁺⁺ ω⁰
5.45 GeV/c
RATIO ρ/ω
b)
c)
|t'| (GeV/c)²

Fig. 22

TECHNICAL INFORMATION DIVISION
LAWRENCE BERKELEY LABORATORY
UNIVERSITY OF CALIFORNIA
BERKELEY, CALIFORNIA 94720